HHS Public Access

Author manuscript

Nat Med. Author manuscript; available in PMC 2015 August 01.

Published in final edited form as:

Nat Med. 2015 February ; 21(2): 132–139. doi:10.1038/nm.3781.

A B cell follicle sanctuary permits persistent productive SIV infection in elite controllers

Yoshinori Fukazawa[1], **Richard Lum**[1], **Afam A. Okoye**[1], **Haesun Park**[1], **Kenta Matsuda**[2], **Jin Young Bae**[1], **Shoko I. Hagen**[1], **Rebecca Shoemaker**[3], **Claire Deleage**[3], **Carissa Lucero**[3], **David Morcock**[3], **Tonya Swanson**[1], **Alfred W. Legasse**[1], **Michael K. Axthelm**[1], **Joseph Hesselgesser**[4], **Romas Geleziunas**[4], **Vanessa M. Hirsch**[2], **Paul T. Edlefsen**[5], **Michael Piatak Jr.**[3], **Jacob D. Estes**[3], **Jeffrey D. Lifson**[3], and **Louis J. Picker**[1,*]

[1]Vaccine and Gene Therapy Institute and Oregon National Primate Research Center, Oregon Health & Science University, Beaverton, Oregon 97006, USA

[2]Laboratory of Molecular Microbiology, National Institute of Allergy and Infectious Diseases, National Institutes of Health, Bethesda, Maryland 20892, USA

[3]AIDS and Cancer Virus Program, Leidos Biomedical Research, Inc., Frederick National Laboratory, Frederick, Maryland 21702, USA

[4]Gilead Sciences, Inc., Foster City, California 94404, USA

[5]Statistical Center for HIV/AIDS Research and Prevention, Vaccine and Infectious Disease Division, Fred Hutchinson Cancer Research Center, Seattle, Washington 98109, USA

Abstract

Chronic phase HIV/SIV replication is reduced by as much as 10,000-fold in elite controllers (EC) compared to typical progressors, but sufficient viral replication persists in EC tissues to allow viral sequence evolution and induce excess immune activation. Here, we show that productive SIV infection in rhesus monkey EC is strikingly restricted to follicular helper $CD4^+$ T cells (T_{FH}), suggesting that while the potent SIV-specific $CD8^+$ T cells of these monkeys can effectively clear productive infection from extra-follicular sites, their relative exclusion from B cell follicles limits elimination of infected T_{FH}. Indeed, $CD8^+$ lymphocyte depletion of EC monkeys resulted in a dramatic re-distribution of productive SIV infection to non-T_{FH}, with T_{FH} restriction resuming upon $CD8^+$ T cell recovery. Thus, B cell follicles constitute sanctuaries for persistent SIV replication in the presence of potent anti-viral $CD8^+$ T cell responses, potentially complicating efforts to cure HIV infection with therapeutic vaccination or T cell immunotherapy.

*To whom correspondence should be addressed (pickerl@ohsu.edu).

AUTHOR CONTRIBUTIONS: LJP and YF conceived the study, designed the experiments and wrote the paper, assisted by AAO, HP, and JDL. YF also supervised the experiments, performed immunologic and SIV co-culture assays, and analyzed the data, assisted by RL, JYB, and SIH. AWL and MKA managed the animal protocols, assisted by TS. KM, VMH, CD, CL, DM and JDE provided tissue-based analysis including immunohistochemistry and RNAscope. MP Jr. and JDL planned and performed SIV quantification assisted by RS. JH and RG developed and provided optimized cART regimens (Cohort #2). PTE performed the statistical analysis of study data.

COMPETING FINANCIAL INTERESTS: The authors declare no competing financial interests.

Introduction

HIV and its nonhuman primate counterpart, SIV, use both specific genetic mechanisms and extraordinary genetic malleability and functional plasticity to either evade or escape innate and adaptive immunity[1,2]. Indeed, the vast majority of infected individuals experience persistent high-level viral replication that in the absence of combination anti-retroviral therapy (cART) leads to AIDS in susceptible species (humans and Asian macaques)[3]. However, rare individuals (<1% for humans) are able to mount highly effective immune responses that suppress viral replication to very low levels, as much as 10,000-fold lower than typical HIV or SIV infections[4,5]. Given the ability of HIV and SIV to establish a stable latent viral reservoir early in infection(6), and the inability of the adaptive immune system to recognize latently infected cells (e.g. cells with integrated viral genomes and no viral gene expression), it is not surprising that the highly effective immune responses developed by EC fail to completely clear HIV/SIV infection. However, it is noteworthy that even these uniquely potent responses are not entirely effective at suppressing ongoing rounds of viral replication. Ultrasensitive analysis reveals detectable plasma virus in most (if not all) ECs at levels that are, on average, higher than those in individuals with infection suppressed by optimal cART); moreover, recovery of replication competent HIV from $CD4^+$ T cells of EC subjects is reduced by cART, and viral sequence analysis indicates that viral replication is high enough to allow for viral sequence evolution[7–12]. EC also manifest higher levels of systemic immune activation than uninfected individuals[13], and this excess immune activation can be reduced by cART[14], findings that taken together provide indirect, but compelling, evidence of persistent, low level productive infection in these subjects.

Highly effective virus-specific $CD8^+$ T cell responses targeting functionally constrained epitopes, typically associated with protective major histocompatibility complex class I alleles, are thought to be responsible for many, if not most, instances of elite HIV and SIV control[4,5,15–18]. The observation that in vivo $CD8^+$ lymphocyte depletion of monkey EC is associated with a rapid upsurge in SIV replication[19], the documentation of immune evolution in EC[9,12], and the ability to isolate replication-competent HIV from human EC[20] all strongly suggest that elite control typically reflects continuous $CD8^+$ T cell-mediated containment of replication-competent virus. If this conclusion is correct, how then does the ongoing low-level productive infection escape the highly effective $CD8^+$ T cell responses? We identified a possible clue to this question in a previous study of live attenuated SIV vaccines (LAV) in rhesus monkeys, in which we demonstrated that SIV-specific T cell responses capable of completely protecting the LAV-vaccinated monkeys from highly pathogenic SIV challenge were continuously maintained by highly restricted LAV replication within the phenotypically distinct $CD4^+$ T_{FH} population in secondary lymphoid tissues[21]. Since most $CD8^+$ effector T cells, including HIV- and SIV-specific $CD8^+$ T cells, lack the appropriate chemokine receptors for B cell follicle entry and therefore are relatively excluded from B cell follicles[22–26], the implication was that the LAV-infected T_{FH} avoided elimination by the highly effective SIV-specific T cells they themselves generated by their location in a B cell follicle “sanctuary”[27]. Indeed, it has been hypothesized that $CD8^+$ T cell exclusion from B cell follicles provides this site with an “immune privilege” that, along with

infection-associated expansion of $CD4^+$ T_{FH}, accounts for preferential viral targeting of $CD4^+$ T_{FH} in progressive HIV/SIV infection[28–33].

In this study, we used SIV infection of Indian-origin rhesus macaques to experimentally assess whether this hypothesized B follicular immune privilege constitutes a substantial barrier to T cell-mediated suppression or clearance of productive lentiviral infection, and might account for persistence of productive SIV infection in elite control. Our data demonstrate that productive SIV infection becomes progressively restricted to $CD4^+$ T_{FH} within B cell follicles with increasing immunologic control, and that this restriction is abruptly abrogated with $CD8^+$ lymphocyte depletion, returning with $CD8^+$ T cell recovery. We also demonstrate preferential localization of residual, productive SIV infection in SIV^+ monkeys with long-term, fully suppressive cART. Taken together, these data confirm that productive SIV infection within resident intrafollicular $CD4^+$ T_{FH} is substantially shielded from $CD8^+$ T cell-mediated suppression or clearance, and that the B cell follicle "sanctuary" this shielding implies will likely constitute a barrier to eradication or functional cure of HIV infection.

Results

Immune control restricts productive SIV infection to T_{FH}

Although $CD4^+$ T_{FH} have been shown to constitute a major, and often disproportionate, component of productively HIV- and SIV-infected cell populations during chronic phase infection, it is unclear whether preferential viral targeting of this subset is based on enhanced susceptibility to infection, a longer intrinsic lifespan of infected cells, location in a particularly conducive environment for productive infection, the relative expansion of $CD4^+$ T_{FH} vs. non-T_{FH} in progressive infection, or preferential shielding of productively infected $CD4^+$ T_{FH} from immune elimination[29–33]. To initially address this question, we quantified replication-competent virus by co-culture analysis of sorted $CD4^+$ T_{FH} vs. non-T_{FH} memory T cells from lymph nodes (LNs) of four rhesus monkeys over the course of controlled LAV (*nef*-deleted SIVmac239) vs. progressive wildtype (WT) SIVmac239 infection. $CD4^+$ T_{FH}, delineated by high co-expression of PD1 and CD200 on $CD4^+$, $CD95^{high}$ memory cells[21,34], were compared to non-T_{FH} $CD4^+$ memory T cells that lacked PD1 and CD200 expression completely ($PD\text{-}1^{neg}/CD200^{neg}$) or expressed these markers at low level ($PD\text{-}1^{dim}/CD200^{dim}$; Suppl. Figs. 1 and 2). During acute LAV infection, and all phases of progressive WT SIV infection, replication-competent virus was present at similar levels in both $CD4^+$ T_{FH} and non-T_{FH} memory T cells (Fig. 1a–c; Suppl. Fig. 3). However, after the onset of immunologic (primarily $CD8^+$ T cell-mediated) control of LAV replication, replication-competent virus could only be isolated from T_{FH} (Fig. 1c). These data suggest that the preferential localization of replication-competent LAV within $CD4^+$ T_{FH} noted in our previous report[21] was related to the development of effective $CD8^+$ T cell responses, which appear to preferentially restrict LAV replication in the T cell zone of the LN paracortex relative to the B cell follicles.

To further explore this possibility and ascertain its applicability to immune control of pathogenic WT SIV infection, we compared the frequency of cells harboring replication-competent SIV^+ and levels of SIV RNA and DNA in $CD4^+$ T_{FH} vs. non-T_{FH} compartments

of LNs from 27 rhesus monkeys chronically infected with WT SIVmac239 or SIVmac251, including ten EC (plasma viral set point ≤600 copies/ml), seven semi-controllers (plasma viral set point between 1,900 and 35,000 copies/ml), and ten typical progressors (plasma viral set points ≥85,000 copies/ml) (Suppl. Table 1). The frequency of T_{FH} within the overall LN $CD4^+$ memory T cell populations of these monkeys reflected their virologic status with EC monkeys manifesting median T_{FH} frequencies of 5% (only slightly higher than uninfected monkeys), semi-controllers 10%, and non-controllers 27% (Fig. 2a,b). Strikingly, and in keeping with the findings in LAV-infected monkeys, monkeys with elite control of WT SIV showed exquisite restriction of replication-competent virus to their very minor population of LN $CD4^+$ T_{FH} (Fig. 2c,d). Of note, levels of replication-competent SIV were similarly low in both the PD-1^-/$CD200^-$ vs. PD-1^{dim}/$CD200^{dim}$ $CD4^+$ memory T cell subsets, suggesting that the ability to host productive SIV infection in EC LN is associated with full T_{FH} differentiation (e.g., a PD-1^{high}/$CD200^{high}$ phenotype) and physical residence in the B cell follicle (see below). Similar restricted localization of replication-competent SIV was observed in splenic $CD4^+$ T_{FH} vs. non-T_{FH} subsets (Suppl. Fig. 4), consistent with restricted viral replication within $CD4^+$ T_{FH} in all secondary lymphoid tissues in these EC monkeys. In contrast, replication-competent SIV was identified at similar levels in $CD4^+$ T_{FH} vs. non-T_{FH} memory T cell subsets in both LNs and spleen from monkeys with progressive infection, whereas semi-controller monkeys were intermediate – showing a variable degree of preferential, but not exclusive, localization of replication-competent SIV in $CD4^+$ T_{FH} vs. non-T_{FH} in LNs and spleen (Fig. 2c,d; Suppl. Fig. 4). Quantification of cell-associated SIV RNA in the $CD4^+$ T_{FH} vs. non-T_{FH} memory T cell subsets from these same monkeys confirmed these results, showing significantly higher SIV RNA content in $CD4^+$ T_{FH} vs. non-T_{FH} in EC and in semi-controllers, but no difference in the SIV RNA content in $CD4^+$ T_{FH} vs. non-T_{FH} in typical progressors (Fig. 2e). These data demonstrate restriction of productive SIV to $CD4^+$ T_{FH} in the presence of immune control, but not its absence. Importantly, levels of cell-associated SIV DNA were only very modestly enriched in $CD4^+$ T_{FH} vs. non-T_{FH} in both EC and semi-controllers (Fig. 2f), suggesting that the mechanism maintaining preferential T_{FH} localization of replication-competent SIV operates primarily, if not exclusively, on productively SIV-infected (SIV antigen-expressing) $CD4^+$ T cells, as would be expected for a $CD8^+$ T cell-mediated process.

Although the phenotypic criteria used to classify and sort $CD4^+$ T_{FH} vs. non-T_{FH} have been anatomically validated (e.g., PD-1^{high}/$CD200^{high}$ $CD4^+$ T cells are exquisitely restricted to B cell follicles; Suppl. Fig. 2), we confirmed the anatomic restriction of productive SIV infection to B cell follicles structures in EC LNs using RNAscope *in situ* hybridization and combined, conventional *in situ* hybridization/immune fluorescence analysis (Fig. 3; Suppl. Figs. 5 and 6). Productively SIV-infected T_{FH} were differentiated from follicular dendritic cell-bound virions by well-described morphologic criteria[31,35]. Consistent with the cell sorting-based assays, we found that a median of 95% of productively SIV-infected cells within the LNs of EC monkeys were localized in B cell follicles (from which $CD8^+$ T cells were largely excluded), whereas in progressors, over half of productively SIV-infected cells were found in the $CD8^+$ T cell-rich paracortex (the latter observation in agreement with our previous study[31]). Thus, using 3 different assays of productive SIV infection – i) frequencies of cells with replication-competent SIV within sorted cell populations, ii) levels of SIV

RNA vs. DNA within sorted cell populations, and iii) anatomic distribution of SIV RNA$^+$ cells by *in situ* analysis – we have shown a striking association between immune control of infection (as reflected by plasma viral set points) and restriction of productive SIV infection to CD4$^+$ T_{FH}.

CD8$^+$ T cells restrict productive SIV infection to T_{FH} in EC

Taken together, these data suggest that the potent SIV-specific CD8$^+$ T cell responses responsible for elite SIV control in rhesus monkeys effectively clear productive SIV infection from the T cell zones of secondary lymphoid tissues, but are unable to completely suppress SIV replication in the CD4$^+$ T_{FH} within B cell follicles. To further test this hypothesis, we monitored the distribution of both replication-competent SIV and SIV RNA and DNA in seven EC monkeys (Suppl. Table 1) following transient *in vivo* CD8$^+$ lymphocyte depletion with the anti-CD8α mAb M-T807R1 (Fig. 4). As expected, mAb M-T807R1 administration completely depleted CD8$^+$ T cells, including SIV-specific CD8$^+$ T cells, from blood and LN by day 10 post-treatment, with partial recovery by day 21 and near maximal recovery by day 35 (Figs. 4a,b). SIV replication dramatically increased and then decreased in close inverse association with CD8$^+$ T cell numbers: plasma viral loads rebounded by nearly 4 logs at the CD8$^+$ T cell nadir (day 10) before being brought back under nearly complete control by day 35 (Fig. 4a). Although NK cells are also depleted by mAb M-T807R1 treatment, these cells are very few in number in LN (Fig. 4c), and in separate studies, we have noted that their efficient depletion by IL-15 blockade is not associated with enhanced SIV replication (Okoye and Picker, unpublished observation), observations that together strongly suggest that the rebound in SIV replication is related to loss of SIV-specific CD8$^+$ T cells rather than NK cells.

Prior to CD8$^+$ lymphocyte depletion, replication-competent SIV was, as described above, highly restricted to the T_{FH} CD4$^+$ subset and CD4$^+$ T cell-associated SIV RNA (but not SIV DNA) was significantly higher in CD4$^+$ T_{FH} vs. non-T_{FH} in EC secondary lymphoid tissues (Fig. 4d–f; Suppl. Fig. 4). However, at day 10 post-CD8$^+$ lymphocyte depletion, replication-competent SIV and cell-associated SIV RNA levels increased dramatically in CD4$^+$ non-T_{FH} (~2 logs for cell-associated SIV RNA) whereas cell-associated SIV DNA levels increased only modestly (~1 log), findings indicating a marked enhancement of productive infection within these cells. CD8$^+$ T cell recovery was associated with a progressive decline in the levels of both replication-competent SIV and cell-associated SIV RNA in the non-T_{FH} CD4$^+$ memory T cells, with pre-depletion levels re-established in most monkeys by day 35 post-depletion and all monkeys by day 84–136 post-depletion (Fig. 4d–f; Suppl. Fig. 7). Although CD8$^+$ lymphocyte depletion also transiently increased levels of cell-associated SIV RNA in CD4$^+$ T_{FH}, the net effect of CD8$^+$ T cell removal was elimination or marked reduction of the pre-depletion disparity in levels of productive SIV infection between CD4$^+$ T_{FH} and non-T_{FH} – the loss of CD8$^+$ T cells having the effect of transiently "converting" EC to progressors in terms of the distribution of productive infection between T_{FH} vs. non-T_{FH} memory CD4$^+$ T cells. The transient equalization of productive SIV infection between CD4$^+$ T_{FH} and non-T_{FH} after the CD8$^+$ lymphocyte depletion was also observed within the spleen (Suppl. Fig. 7), suggesting this was a general effect in all secondary lymphoid tissues.

$CD8^+$ lymphocyte depletion has secondary effects on $CD4^+$ memory T cell homeostasis, in particular the enhancement of $CD4^+$ memory T cell proliferation[36]. To determine whether induction of homeostatic proliferation of non-T_{FH} may have played a role in the equalization of replication-competent SIV levels in $CD4^+$ T_{FH} and non-T_{FH}, we determined the effect of artificially inducing non-T_{FH} $CD4^+$ memory T cell proliferation using a non-$CD8^+$ lymphocyte-depleting mechanism – IL-7 administration[37] – on the distribution of replication-competent SIV within LN $CD4^+$ T cell compartments of EC monkeys. Administration of two doses of recombinant IL-7 (30 μg/kg) induced levels of proliferation (%Ki-67^+) among non-T_{FH} $CD4^+$ T cells comparable to those induced by $CD8^+$ lymphocyte depletion (Fig. 5a). However, this treatment had no effect on the plasma viral load or, most importantly, on the highly restricted localization of replication-competent SIV in T_{FH} in these EC monkeys (Fig. 5b,c). Taken together, these data support a $CD8^+$ T cell-mediated mechanism for the transient equalization of productive SIV infection between $CD4^+$ T_{FH} and non-T_{FH} after $CD8^+$ lymphocyte depletion of EC monkeys, and in these monkeys, strongly point to a differential ability of their highly effective SIV-specific $CD8^+$ T cells to clear productive SIV infection of $CD4^+$ memory T cells within the T cell zones vs. B follicles of their secondary lymphoid tissues.

T_{FH} preferentially harbor productive SIV infection after cART

The apparent ability of B follicular structures to substantially shield productively SIV-infected $CD4^+$ T_{FH} from $CD8^+$ T cell-mediated clearance raises the question of whether this mechanism might counter the ability of spontaneous or therapeutic vaccine-induced $CD8^+$ T cell responses to eradicate or functionally cure HIV/SIV infection in the setting of effective pharmacologic viral suppression[6]. Given the data described above, we would predict that if viral reactivation or residual viral replication occurs in $CD4^+$ T_{FH} within the secondary lymphoid tissues of individuals on cART, it would be relatively protected from clearance by such $CD8^+$ T cell responses. Moreover, it is possible that even the conventional (less effective than EC) virus-specific $CD8^+$ T cell responses present in typical individuals on cART might be able to generate sufficient $CD8^+$ T cell-mediated immune pressure to restrict productive HIV/SIV infection arising from reactivation or residual replication in these individuals to the protected environment of the B cell follicle. To determine whether SIV reactivation or residual replication within $CD4^+$ memory T cells was differentially distributed between the extra-follicular T cell zone and B cell follicles in the setting of pharmacologically suppressed SIV infection, we determined the levels of SIV RNA and DNA within $CD4^+$ T_{FH} and non-T_{FH} cells in two different cohorts of monkeys with progressive or semi-controlled SIV infection that were treated with cART for at least four months, all with plasma viral loads at the time of testing ≤60 copies/ml (Suppl. Table 2; note that the level of productive SIV infection in these cART-suppressed monkeys was below the level of detection of our co-culture assay). In Cohort #1, LN and splenic $CD4^+$ T_{FH} and non-T_{FH} were sorted on the basis of PD-1 and CD200 expression, as described above; in Cohort #2, LN $CD4^+$ T_{FH} were sorted on the basis of PD-1 and CXCR5 expression, and the $CD4^+$ non-T_{FH} were separated into the traditional central memory (T_{CM}) and transitional effector memory ($T_{Tr/EM}$) subsets on the basis of CD28, CCR5, and CCR7 expression[3] (Suppl. Fig. 8). As shown in Fig. 6a–c, cell-associated SIV RNA, but not SIV DNA, was significantly higher in $CD4^+$ T_{FH}, compared to non-T_{FH} in both cohorts, consistent with preferential

localization of residual productive SIV infection within the B cell follicles of secondary lymphoid tissues in the majority of cART-treated monkeys. Although T_{FH} constitute only a median of 12% of total $CD4^+$ memory T cells within LNs of these cART-suppressed monkeys (Fig. 2a,b), these data indicate that a substantial fraction of viral reactivation or residual viral replication in effectively cART-treated monkeys occurs with the protected environment of the B cell follicle.

DISCUSSION

These studies indicate that in the absence of strong $CD8^+$ T cell-mediated immune control – either typical progressive SIV infection or controlled SIV infection after $CD8^+$ lymphocyte depletion – there are only minor differences in the levels of productive SIV infection between T_{FH} and non-T_{FH} $CD4^+$ memory T cells; whereas in the presence of such control (particularly in elite control; e.g., plasma viral load set points of $<10^3$ SIV RNA copies/ml), there is marked restriction of productive SIV infection to $CD4^+$ T_{FH} by both phenotypic and anatomic criteria. Thus, for the first time, we directly demonstrate that $CD8^+$ T cell-mediated control of SIV infection is linked to restriction in the anatomic location of productive infection, and that B cell follicles constitute a sanctuary for residual productive SIV infection in the face of highly effective $CD8^+$ T cell responses. While this novel immune avoidance mechanism is likely dispensable at the viral replication rates associated with untreated progressive infection, it becomes clinically relevant in elite control, almost certainly playing a major role in the persistence of productive infection in this setting. Whether fortuitous or a reflection of evolutionary adaptation, the ability of SIV to exploit a B follicular sanctuary to avoid highly effective $CD8^+$ T cell effector responses constitutes a potentially important immune evasion strategy for the virus, because it provides for viral replication rates sufficient to allow for viral sequence evolution[9,12], and the possibility of eventual immune escape. In contrast, if highly effective virus-specific $CD8^+$ T cell responses were able to drive the infection into full latency, such evolution and consequent escape could not occur.

In keeping with the general exclusion of most $CD8^+$ T cells from B cell follicles[22,23], previous studies have established that in HIV or SIV infection B cell follicles have reduced frequencies of HIV- and SIV-specific $CD8^+$ T cells compared to extra-follicular sites[24–26]. This finding suggests that the B follicular sanctuary defined in this study might result from the normal physiologic regulation of follicular homing that limits $CD8^+$ effector T cell migration into B cell follicles, and thereby would compromise $CD8^+$ T cell-mediated anti-viral activity in these structures. In addition, it is possible that the “per cell” anti-viral effector capabilities of the few $CD8^+$ effector T cells that enter the follicle are less than those of their extra-follicular counterparts[38], and/or that SIV-infected $CD4^+$ T_{FH} are more resistant to their effector activity. Importantly, however, this “shielding” of SIV-infected cells within B cell follicles from $CD8^+$ T cell effector function must be relative, rather than absolute, as the transient increase in productively SIV-infected $CD4^+$ T_{FH} after $CD8^+$ lymphocyte depletion (Fig. 4) indicates that $CD4^+$ T_{FH} infection is at least partially limited by effective $CD8^+$ T cell responses. This control might result from distant effects of extra-follicular $CD8^+$ T cells (potentially limiting entry of infected pre-T_{FH} into the follicle), or to the few $CD8^+$ T cells that gain follicular homing function[23,38]. Interestingly, chronic

progressive HIV infection is associated with increased numbers of $CD8^+$ T cells in B cell follicles[39–41], and expansion of $CD8^+$ effector T cells expressing a $CCR7^{low}$ $CXCR5^{high}$ "follicle homing" phenotype[42]. Thus, the normal relative exclusion of $CD8^+$ effector T cells from B cell follicles is ultimately compromised during the transition from follicular hyperplasia to follicular lysis, and ultimately, follicular involution and atrophy that characterizes progressive HIV disease[35]. However, the increased follicular localization of $CD8^+$ T cells in this situation (progressive infection) occurs in the absence of effectively anti-viral $CD8^+$ T cell responses, and therefore likely contributes more to pathogenesis (inflammatory destruction of lymphoid architecture) than to viral control. Follicular integrity (operationally defined as the relative exclusion of $CD8^+$ T cells from B cell follicles) is not compromised in elite control (Fig. 3 and Suppl. Fig. 5), and therefore in this setting, follicular structure and/or the normal physiology of follicular migration would protect productively SIV-infected $CD4^+$ T_{FH} from $CD8^+$ T cell-mediated clearance. Although our data do not definitively implicate the activity of SIV-specific $CD8^+$ T cells in the preferential localization of SIV RNA^+ cells in $CD4^+$ T_{FH} in monkeys with cART-suppressed infection, follicular integrity is largely intact in the LNs of these monkeys (Suppl. Fig. 9), and thus, it is highly likely that the B cell follicle sanctuary operates in this setting as well (at least with cART initiation prior to the infection-associated destruction of LN architecture).

It is generally accepted that eradication or functional cure of HIV infection will almost certainly require both the induction of latent virus, and immune-mediated destruction of the cells hosting the resultant viral reactivation[6,43]. The clinical implication of our findings is that intrafollicular $CD4^+$ T cells (T_{FH}) appear to comprise a substantial fraction of virally infected cells in the setting of cART-suppressed infection, and therefore, the B cell follicle sanctuary will likely constitute a formidable barrier to the use of spontaneous or vaccine-elicited $CD8^+$ T cell responses to either clear HIV reservoirs or fully suppress HIV reactivation after cART cessation. Indeed, it might prove necessary to add a third component to HIV cure strategies that rely on $CD8^+$ T cell responses to destroy HIV $antigen^+$ cells after latent virus reactivation – temporary disruption of B follicular integrity, perhaps using transient B cell depletion (e.g., anti-CD20 antibody therapy) or immunomodulation strategies (e.g., CD40L blockade)[44]. Alternatively, it might be possible to develop vaccines or other immunotherapies that can generate $CD8^+$ T cell effector responses that can efficiently penetrate and work within the B follicular environment[23,38,42]. In this regard, it is noteworthy that we have previously demonstrated one situation – prophylactic vaccination with CMV vectors expressing SIV proteins – in which a widely distributed, albeit very early, SIV infection can be cleared over time by an effector memory T cell-mediated mechanism[45]. In this situation, either the vaccine-generated SIV-specific effector memory T cell responses (which include both $CD4^+$ and $CD8^+$ components) were able to control infection prior to $CD4^+$ T_{FH}/B cell follicle seeding, or these responses had an ability to penetrate B cell follicles and eliminate virally infected cells therein.

In conclusion, we have demonstrated that SIV can take advantage of the relative exclusion of $CD8^+$ effector T cells from B cell follicles to persist and preferentially replicate within $CD4^+$ T_{FH} cells when $CD8^+$ T cell-mediated immune pressure is high, thereby escaping even the highly potent $CD8^+$ T cell responses that develop in EC. Since both follicular

exclusion of human $CD8^+$ T cells and the ability of human $CD4^+$ T_{FH} to support HIV infection are well-documented[24,29], this mechanism is very likely to operate in HIV-infected humans as well. Therefore, therapies intended to eradicate HIV infection will almost certainly need to overcome the B follicular sanctuary.

FULL METHODS

Animals and viruses

This study used 50 purpose-bred adult rhesus macaques (*Macaca mulatta*) of Indian genetic background (39 males/11 females; age range: 4–17 years), all of which were free of cercopithicine herpesvirus 1, D type simian retrovirus, and simian T-lymphotrophic virus type 1 at the start of the study. We studied 46 monkeys at the Oregon National Primate Research Center with the approval of the Oregon National Primate Research Center Institutional Animal Care and Use Committee, under the standards of the NIH Guide for the Care and Use of Laboratory Animals. We also studied four rhesus macaques (SIV-infected progressors) that were housed at the National Institutes of Health in accordance with the same standards under the approval by the Institutional Animal Care and Use Committee of the National Cancer Institute. All rhesus macaques were infected with SIVmac239, SIVmac251, or with LAV (SIVmac239Δnef) (see Suppl. Table 1). We $CD8^+$ lymphocyte-depleted seven EC monkeys in chronic phase of WT SIV infection (191–967 days post-infection) with anti-CD8 monoclonal antibody (mAb) M-T807R1 (National Institutes of Health Nonhuman Primate Reagent Resource Program, Boston, MA.)[36]. M-T807R1 was injected subcutaneously (10 mg/kg) at day 0, and intravenously (5 mg/kg) at days 3, 7, and 10. After the recovery of $CD8^+$ lymphocyte depletion (5–6 months after the antibody treatment), we administered two subcutaneous injections of recombinant simian IL-7 (30 μg/kg each, Cytheris) at days 0 and 7 as described[37] to three of the previously $CD8^+$ cell-depleted monkeys (Rh25610, Rh25687, Rh26623). We used the cART regimen described below to suppress SIV replication in 17 WT SIV-infected monkeys (see Suppl. Table 2).

Cell processing

Mononuclear cell preparations were obtained from blood, LN, and spleen, as previously described[21,45]. $CD4^+$ memory T cell subsets were isolated from LN or spleen by sorting on a FACS Aria II (BD Biosciences) on the basis of cell surface staining patterns (lineage markers CD3 and CD4, memory markers CD95 and CD28, and T_{FH} markers PD-1 and CD200) after excluding dead cells (LiVEDEAD® Fixable Aqua Dead Cell Stain Kits, Invitrogen), as shown in Suppl. Fig. 1. In some experiments, $CD4^+$ memory T cell subset (T_{CM}, $T_{Tr/EM}$, and T_{FH}) cells were sorted as shown in Suppl. Fig. 8. To determine the phenotype of T cells and to sort $CD4^+$ memory T cell subsets, these antibodies were used; CD3 (SP34-2, BD), CD4 (L200, BD), CD8 (DK25, Dako), CD8a (SK1, BD), CD200 (OX104, BioLegend), CD95 (DX2, eBioscience), CD28 (28.2, BD), PD-1 (J105, eBioscience), CXCR5 (MU5UBEE, eBioscience), CCR7 (15053, R&D Systems), and CCR5 (3A9, BD).

Viral quantification

Replication-competent SIV was rescued from graded numbers of sorted $CD4^+$ memory T cell subsets (10^3, 10^4, or 10^5 cells) by the co-cultivation of these sorted cells with CEMx174 cells (10^5 cells, NIH AIDS Reagent Program) in 24-well plates, followed by flow cytometric analysis of intracellular SIV-Gag p27 expression [with anti-CD3 (SP34-2) and anti-CD4 (L200), anti-Gag p27 (55-2F12, NIH AIDS Research and Reference Reagent Program) antibodies were used to detect viral replication in CEMx174], as described[21]. Co-cultured cells were harvested and analyzed at days 13 to 36, with quantitative comparisons of the extent of infection in co-cultures containing different $CD4^+$ memory T cell populations performed at the earliest time point of maximum expression of Gag p27 in the co-cultures of any of the three $CD4^+$ memory T cell subsets. For cell-associated viral load determination, sorted $CD4^+$ memory T cell subsets from LN were pelleted and frozen immediately and stored at −80 °C until use for quantitative PCR/RT-PCR. Quantitative PCR and RT-PCR assays targeting a highly conserved nucleic acid sequence in *gag* were used for standard measurement of plasma SIV RNA and cell-associated SIV RNA/DNA in sorted $CD4^+$ memory T cell subsets isolated from LN, as previously described (with cell-associated SIV RNA/DNA normalized to co-determined cell equivalents based on quantitation of 2 copies of CCR5 sequence per cell)[46,47].

SIV-specific T cell response assays

SIV-specific $CD8^+$ T cells were quantified in mononuclear cells isolated from blood and LN by flow cytometric intracellular cytokine analysis, as previously described in detail[45]. Briefly, mixes of sequential (11 amino acid overlapping) 15-mer peptides (AnaSpec) spanning the SIVmac239 Gag, Env, Pol, Nef, Rev/Tat, Vif/Vpr/Vpx proteins were used as antigens in conjunction with anti-CD28 (BD Biosciences) and anti-CD49d co-stimulatory mAb (BD Biosciences). Cells were incubated at 37 °C with peptide mixes/pools and co-stimulatory antibodies for 1 hr, followed by an additional 8 hr. incubation in the presence of Brefeldin A (5 μg/ml, Sigma-Aldrich). Co-stimulation in the absence of peptides served as background control. Cells were stained with fluorochrome-conjugated monoclonal antibodies [CD3 (SP34-2), CD4 (L200), CD8a (SK1), IFN-γ (B27)(BD Biosciences), TNF (MAB11, eBioscience), CD69 (FN50, BD Biosciences)], and data were collected on an LSRII (BD Biosciences) and analyzed using the FlowJo software program (version 8.8.7; Tree Star, Inc.). Response frequencies to each peptide mix were defined by the intracellular expression of TNF and/or IFN-γ by $CD3^+$, $CD4^-$, $CD8^+$ T cells after subtraction of background. Response frequencies to each peptide mix were added to obtain total SIV-specific response frequencies.

Immunofluorescence confocal microscopy

Tissue sections (5 μm) were mounted on Superfrost Plus Microscope Slides (Fisher Scientific), heated at 60°C for 1h, dewaxed in xylenes and rehydrated in graded ethanols and double-distilled H_2O. Heat-induced epitope retrieval was performed by heating sections in 0.01% citraconic anhydride containing 0.05% Tween-20 in a pressure cooker set at 122 °C for 30 sec. Tissues were blocked in blocking buffer [TBS containing 0.05% Tween-20 (TBS-Tw) and 0.25% casein] for 10 min at room temperature and then incubated with

mouse anti-CD4 (clone 1F6; 1:25; Vector Labs), goat anti-PD1 (1:200; R&D Systems; AF1086) and rabbit anti-CD200 (1:200; Sigma; HPA031149) diluted in blocking buffer overnight at room temperature. Slides were washed in TBS-Tw and incubated with donkey anti-mouse-Alexa488, donkey anti-goat–Alexa647, and donkey anti-rabbit–Alexa594 (all Invitrogen; 1:400) for 1h at room temperature in the dark and washed in TBS-Tw. Slides were incubated with 0.1% Sudan Black B in 70% ethanol (Cat. No. 4410; ENG Scientific) for 30 min at room temperature to quench autofluorescence then incubated with 300 nM DAPI for 10 min. Slides were washed, mounted with Prolong® Gold (Invitrogen) and imaged on an Olympus FV10i confocal microscope using a 10x phase contrast objective (NA 0.4) with 2x Optical zoom using sequential mode to separately capture the fluorescence from the different fluorochromes at an image resolution of 1024x1024 pixels.

Fluorescent immunohistochemistry (FIHC) and fluorescent *in situ* hybridization (FISH)

SIV RNA$^+$, CD8$^+$, and CD20$^+$ cells were detected in 4% PFA-fixed, paraffin-embedded LN sections by a combination of FIHC and FISH assays with a previously described modified method[48]. Briefly, the sections were treated with methanol-hydrogen peroxide then hybridized overnight at 45 °C with antisense SIVmac239 digoxigenin-UTP-labeled riboprobe. The hybridized sections were blocked with 3% normal sheep (Jackson ImmunoResearch Laboratories) and horse serum (Sigma-Aldrich) in 0.1 M Tris, pH7.4, and then incubated with sheep anti-digoxigenin-horseradish peroxidase (SAD-POD; Roche Applied Science). SAD-POD was detected by a fluorescent tyramide signal amplification technique (TSA Plus Fluorescein Kit; PerkinElmer). After completion of the FISH assay, the sections were incubated in mouse anti-human CD20 monoclonal antibody (Clone L26; Thermo Scientific), followed by incubation with goat anti-mouse IgG-Biotinylated antibody (Vector Laboratories) and then stained with Streptavidin Alexa-647 conjugate (Life Technologies). The double-stained sections were then incubated with rabbit anti-human CD8 monoclonal antibody (Clone SP16; Thermo Scientific), followed by Alexa 594-conjugated goat anti-rabbit IgG antibody (Life Technologies). The triple-stained sections were mounted in ProLong Gold antifade reagent (Life Technologies). All confocal images were acquired using a Leica TCS SP8 confocal microscope (Leica Microsystems) equipped with a 20x/NA 0.75 oil immersion objective. Large field images of the tissue sections were generated by assembly of numerous juxtaposed individual sub-images into a montage, assisted by Fiji software (http://fiji.sc/wiki/index.php/Fiji).

RNAscope analysis

We also utilized a novel next-generation, ultrasensitive RNA *in situ* hybridization technology, RNAscope, for SIV *in situ* hybridization, as previously described[49]. Quantification of the number of productively infected SIV RNA$^+$ cells either within or outside follicles was performed by manual counting of high magnification whole Aperio scanned tissue sections using the Aperio elliptical annotation tool independently by three blinded individuals. Productively infected SIV RNA$^+$ cells were classified based on an intense centric SIV RNA signal within a single cell (both nuclear and cytoplasmic) that diffused toward the edges of the cell, which is distinguished from the “lattice-like” filamentous pattern of extracellular FDC-bound virus that is seen within the follicles[31]. The average fraction of productively infected SIV RNA$^+$ cells within the B cell follicles is

reported for EC vs. progressors (total productively infected SIV RNA$^+$ cells counted: 245 for EC; 1,252 for progressors).

Combination antiretroviral therapy (cART)

For Cohort 1 (Supplementary Table 2), cART consisted of subcutaneously injected 20mg/kg^{-1} d^{-1} tenofovir (TFV) and 50 mg/kg^{-1} d^{-1} emtricitabine (FTC), and orally administered (given in food) 240 mg/kg^{-1} d^{-1} raltegravir and 600 mg darunavir twice daily boosted with 100 mg ritonavir twice daily. All Cohort 1 monkeys had been chronically infected with SIVmac251 at the time of cART initiation and were treated with the cART for a minimum of 18 weeks. For Cohort 2, cART consisted of 20 mg/kg^{-1} d^{-1} TFV, 50 mg/kg^{-1} d^{-1} FTC, 2.5 mg/kg^{-1} d^{-1} dolutegravir (DTG; all given as a single subcutaneous injection) and 600?mg darunavir twice daily boosted with 100?mg ritonavir twice daily (given orally in food). Daily darunavir and ritonavir (Oregon Health & Science University pharmacy) were stopped after 96 days. All Cohort #2 monkeys had been infected with SIVmac239 prior to ART initiation at day 42 post-infection, and treated with cART for 26 weeks at the time of biopsy. The injectable component of the cART regimen was composed of 20 mg/mL TFV, 50 mg/mL FTC, and 2.5 mg/mL DTG in a solvent containing 25% (v/v) polyethylene glycol 400 (PEG-400), 15% (w/v) captisol and 0.075 N sodium hydroxide (NaOH) in water. The injectable cART formulation was prepared by mixing DTG stock solution (10 mg/mL in PEG-400), TFV stock solution (80 mg/mL in 0.3 N NaOH), FTC stock solution (200 mg/mL in 0.3 N NaOH), and 30% (w/w) captisol solution at a 1:1:2 (v:v:v) ratio. The final solution had a pH ~6, was sterile-filtered, aliquoted into sterile glass vials and frozen at −20°C until used. This injectable component of the cART regimen was administered subcutaneously once daily at 1 mL/kg body weight.

Statistical analysis

We conducted all statistical analyses without multiplicity correction, using nonparametric, two-sided tests[50]. Study animals were selected for inclusion in the study based on pre-specified criteria and these selected animals contributed data to all analyses. The only exceptions to this were instances when insufficient sorted cells could be recovered from available tissue samples, resulting in some variability in the group size across the various analyses. Because the animal groups were defined by controller status or ART status, no randomization was used, and no blinding was performed. To compare cell-associated viral DNA, RNA, or percentage of SIV-Gag p27 in CEMx174, within-animal differences across CD4$^+$ memory subsets based on PD-1 and CD200 expression (PD-1$^-$/CD200$^-$, PD-1^{dim}/CD200$^{-\text{ to dim}}$, PD-1^{high}/CD200^{high}; Suppl. Fig. 1) or other differentiation markers (T_{CM}, $T_{Tr/EM}$, T_{FH}; Suppl. Fig. 8), we conducted Friedman tests (non-parametric randomized block ANOVA) at the 0.05 significance level. For pairwise comparisons between categories of within-animal differences, we applied the Wilcoxon signed-rank test (at the 0.05 level). For comparisons across groups of animals we applied 0.05-level Kruskal-Wallis and Wilcoxon rank-sum tests (for >2 and 2 groups, respectively). We used the R statistical computing language for all statistical analyses[51].

Supplementary Material

Refer to Web version on PubMed Central for supplementary material.

Acknowledgments

This work was supported by the US National Institutes of Health, including grants 4R37A1054292 (LJP), 1U19AI096109 (LJP and AAO), and 8P51OD01109255, contract HHSN261200800001E (JDE) and Intramural Program of the US National Institute of Allergy and Infectious Diseases, and the Bill and Melinda Gates Foundation (grant #41185; LJP). The authors thank Drs. R. Wiseman and D. Watkins for major histocompatibility complex typing, Dr. K. Reimann and the US National Institutes of Health's Nonhuman Primate Reagent Resource Program for provision of the CD8α-specific monoclonal antibody M-T807R1, Dr. D. Hazuda (Merck Research Labs) for providing cART drugs for Cohort #1, Cytheris SA (Issy Les Moulineaux, France) for recombinant rhesus IL-7, Dr. S. Hansen for animal study management, Dr. A. Sylwester, L. Koo, J. Clock, A. Konfe, H.W. Kim, M. Rohankhedkar, M. Reyes, N. Coombes, B. Assaf, K. Oswald, R. Fast, Y. Li, C. Trubey, J. Turner, S. Planer and L. Boshears for technical or administrative assistance.

References

1. Kirchhoff F. Immune evasion and counteraction of restriction factors by HIV-1 and other primate lentiviruses. Cell Host Microbe. 2010; 8:55–67. [PubMed: 20638642]
2. Picker LJ, Hansen SG, Lifson JD. New paradigms for HIV/AIDS vaccine development. Annu Rev Med. 2012; 63:95–111. [PubMed: 21942424]
3. Okoye AA, Picker LJ. CD4(+) T-cell depletion in HIV infection: mechanisms of immunological failure. Immunol Rev. 2013; 254:54–64. [PubMed: 23772614]
4. Deeks SG, Walker BD. Human immunodeficiency virus controllers: mechanisms of durable virus control in the absence of antiretroviral therapy. Immunity. 2007; 27:406–416. [PubMed: 17892849]
5. Mudd PA, Watkins DI. Understanding animal models of elite control: windows on effective immune responses against immunodeficiency viruses. Curr Opin HIV AIDS. 2011; 6:197–201. [PubMed: 21502922]
6. Katlama C, et al. Barriers to a cure for HIV: new ways to target and eradicate HIV-1 reservoirs. Lancet. 2013; 381:2109–2117. [PubMed: 23541541]
7. Hatano H, et al. Evidence for persistent low-level viremia in individuals who control human immunodeficiency virus in the absence of antiretroviral therapy. J Virol. 2009; 83:329–335. [PubMed: 18945778]
8. Pereyra F, et al. Persistent low-level viremia in HIV-1 elite controllers and relationship to immunologic parameters. J Infect Dis. 2009; 200:984–990. [PubMed: 19656066]
9. Bailey JR, Williams TM, Siliciano RF, Blankson JN. Maintenance of viral suppression in HIV-1-infected HLA-B*57^{+} elite suppressors despite CTL escape mutations. J Exp Med. 2006; 203:1357–1369. [PubMed: 16682496]
10. Chun TW, et al. Effect of antiretroviral therapy on HIV reservoirs in elite controllers. J Infect Dis. 2013; 208:1443–1447. [PubMed: 23847057]
11. Mens H, et al. HIV-1 continues to replicate and evolve in patients with natural control of HIV infection. J Virol. 2010; 84:12971–12981. [PubMed: 20926564]
12. O'Connell KA, et al. Control of HIV-1 in elite suppressors despite ongoing replication and evolution in plasma virus. J Virol. 2010; 84:7018–7028. [PubMed: 20444904]
13. Hunt PW, et al. Relationship between T cell activation and CD4^{+} T cell count in HIV-seropositive individuals with undetectable plasma HIV RNA levels in the absence of therapy. J Infect Dis. 2008; 197:126–133. [PubMed: 18171295]
14. Hatano H, et al. Prospective antiretroviral treatment of asymptomatic, HIV-1 infected controllers. PLoS Pathog. 2013; 9:e1003691. [PubMed: 24130489]
15. Walker BD, Yu XG. Unravelling the mechanisms of durable control of HIV-1. Nat Rev Immunol. 2013; 13:487–498. [PubMed: 23797064]
16. Saez-Cirion A, Pancino G. HIV controllers: a genetically determined or inducible phenotype? Immunol Rev. 2013; 254:281–294. [PubMed: 23772626]

17. Mendoza D, et al. Cytotoxic capacity of SIV-specific CD8(+) T cells against primary autologous targets correlates with immune control in SIV-infected rhesus macaques. PLoS Pathog. 2013; 9:e1003195. [PubMed: 23468632]
18. Mudd PA, et al. Reduction of $CD4^+$ T cells *in vivo* does not affect virus load in macaque elite controllers. J Virol. 2011; 85:7454–7459. [PubMed: 21593153]
19. Friedrich TC, et al. Subdominant $CD8^+$ T-cell responses are involved in durable control of AIDS virus replication. J Virol. 2007; 81:3465–3476. [PubMed: 17251286]
20. Blankson JN, et al. Isolation and characterization of replication-competent human immunodeficiency virus type 1 from a subset of elite suppressors. J Virol. 2007; 81:2508–2518. [PubMed: 17151109]
21. Fukazawa Y, et al. Lymph node T cell responses predict the efficacy of live attenuated SIV vaccines. Nat Med. 2012; 18:1673–1681. [PubMed: 22961108]
22. Crotty S. Follicular helper CD4 T cells (TFH). Ann Rev Immunol. 2011; 29:621–663. [PubMed: 21314428]
23. Vinuesa CG, Cyster JG. How T cells earn the follicular rite of passage. Immunity. 2011; 35:671–680. [PubMed: 22118524]
24. Connick E, et al. CTL fail to accumulate at sites of HIV-1 replication in lymphoid tissue. J Immunol. 2007; 178:6975–6983. [PubMed: 17513747]
25. Tjernlund A, et al. In situ detection of Gag-specific $CD8^+$ cells in the GI tract of SIV infected Rhesus macaques. Retrovirology. 2010; 7:12. [PubMed: 20158906]
26. Sasikala-Appukuttan AK, et al. Location and dynamics of the immunodominant CD8 T cell response to SIVDeltanef immunization and SIVmac251 vaginal challenge. PloS one. 2013; 8:e81623. [PubMed: 24349100]
27. Robinson HL, Amara RR. Protective immunity from a germinal center sanctuary. Nat Med. 2012; 18:1614–1616. [PubMed: 23135510]
28. Skinner PJ, Connick E. Overcoming the immune priviledge of B-cell follicles to cure HIV-1 infection. J Hum Virol Retrovirol. 2014; 1(1):00001.10.15406/jhvrv.2014.01.00001
29. Perreau M, et al. Follicular helper T cells serve as the major CD4 T cell compartment for HIV-1 infection, replication, and production. J Exp Med. 2013; 210:143–156. [PubMed: 23254284]
30. Lindqvist M, et al. Expansion of HIV-specific T follicular helper cells in chronic HIV infection. J Clin Invest. 2012; 122:3271–3280. [PubMed: 22922259]
31. Brenchley JM, et al. Differential infection patterns of $CD4^+$ T cells and lymphoid tissue viral burden distinguish progressive and nonprogressive lentiviral infections. Blood. 2012; 120:4172–4181. [PubMed: 22990012]
32. Petrovas C, et al. CD4 T follicular helper cell dynamics during SIV infection. J Clin Invest. 2012; 122:3281–3294. [PubMed: 22922258]
33. Klatt NR, et al. SIV infection of rhesus macaques results in dysfunctional T- and B-cell responses to neo and recall Leishmania major vaccination. Blood. 2011; 118:5803–5812. [PubMed: 21960586]
34. Chtanova T, et al. T follicular helper cells express a distinctive transcriptional profile, reflecting their role as non-Th1/Th2 effector cells that provide help for B cells. J Immunol. 2004; 173:68–78. [PubMed: 15210760]
35. Estes JD. Pathobiology of HIV/SIV-associated changes in secondary lymphoid tissues. Immunol Rev. 2013; 254:65–77. [PubMed: 23772615]
36. Okoye A, et al. Profound $CD4^+/CCR5^+$ T cell expansion is induced by $CD8^+$ lymphocyte depletion but does not account for accelerated SIV pathogenesis. J Exp Med. 2009; 206:1575–1588. [PubMed: 19546246]
37. Leone A, et al. Increased $CD4^+$ T cell levels during IL-7 administration of antiretroviral therapy-treated simian immunodeficiency virus-positive macaques are not dependent on strong proliferative responses. J Immunol. 2010; 185:1650–1659. [PubMed: 20622118]
38. Quigley MF, Gonzalez VD, Granath A, Andersson J, Sandberg JK. $CXCR5^+$ $CCR7^-$ CD8 T cells are early effector memory cells that infiltrate tonsil B cell follicles. Eur J Immunol. 2007; 37:3352–3362. [PubMed: 18000950]

39. Wood GS, Garcia CF, Dorfman RF, Warnke RA. The immunohistology of follicle lysis in lymph node biopsies from homosexual men. Blood. 1985; 66:1092–1097. [PubMed: 3876855]
40. Tenner-Racz K, et al. Monoclonal antibodies to human immunodeficiency virus: their relation to the patterns of lymph node changes in persistent generalized lymphadenopathy and AIDS. AIDS. 1987; 1:95–104. [PubMed: 3130085]
41. Tenner-Racz K, et al. Cytotoxic effector cell granules recognized by the monoclonal antibody TIA-1 are present in $CD8^+$ lymphocytes in lymph nodes of human immunodeficiency virus-1-infected patients. Am J Pathol. 1993; 142:1750–1758. [PubMed: 8506945]
42. Petrovas, C., et al. A population of $CD8^+$ T cells located in germinal centers that is functionally capable of mediating bispecific antibody killing of HIV-infected T cells. 20th International AIDS Conference; Melbourne, Australia. 2014. http://pag.aids2014.org/Abstracts.aspx?SID=1147&AID=5387
43. Shan L, et al. Stimulation of HIV-1-specific cytolytic T lymphocytes facilitates elimination of latent viral reservoir after virus reactivation. Immunity. 2012; 36:491–501. [PubMed: 22406268]
44. Anolik JH, Aringer M. New treatments for SLE: cell-depleting and anti-cytokine therapies. Best Prac & Res Clin Rheum. 2005; 19:859–878.
45. Hansen SG, et al. Immune clearance of highly pathogenic SIV infection. Nature. 2013; 502:100–104. [PubMed: 24025770]
46. Cline AN, Bess JW, Piatak M Jr, Lifson JD. Highly sensitive SIV plasma viral load assay: practical considerations, realistic performance expectations, and application to reverse engineering of vaccines for AIDS. J Med Primatol. 2005; 34:303–312. [PubMed: 16128925]
47. Venneti S, et al. Longitudinal in vivo positron emission tomography imaging of infected and activated brain macrophages in a macaque model of human immunodeficiency virus encephalitis correlates with central and peripheral markers of encephalitis and areas of synaptic degeneration. Am J Pathol. 2008; 172:1603–1616. [PubMed: 18467697]
48. Brown CR, et al. Unique pathology in simian immunodeficiency virus-infected rapid progressor macaques is consistent with a pathogenesis distinct from that of classical AIDS. J Virol. 2007; 81:5594–5606. [PubMed: 17376901]
49. Smedley J, et al. Tracking the luminal exposure and lymphatic drainage pathways of intravaginal and intrarectal inocula used in nonhuman primate models of HIV transmission. PloS one. 2014; 9:e92830. [PubMed: 24667371]
50. Wolfe, MHDA. Nonparametric Statistical Methods. John Wiley & Sons; New York: 1999.
51. R Core Team. R: a language and environment for statistical computing. R Foundation for Statistical Computing; Vienna, Austria: 2014. <http:/www.r-project.org/>

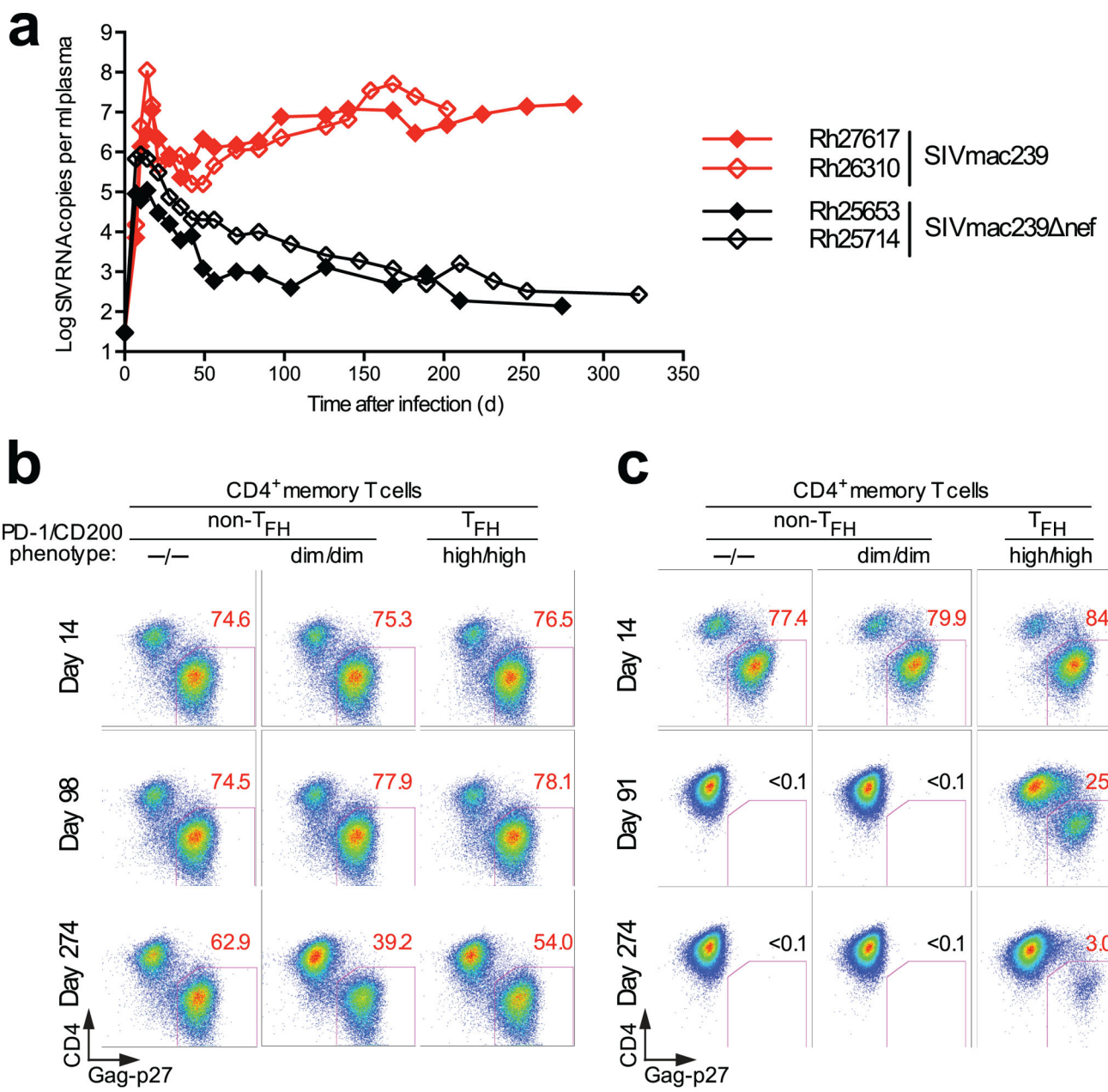

Figure 1. Levels of productive SIV infection within CD4$^+$ memory T cell subsets differ in chronic phase attenuated vs. wildtype (WT) SIVmac239 infection

(**a**) Plasma viral load profiles of representative SIVmac239 and SIVmac239Δnef infections. (**b,c**) Detection of replication-competent SIV within PD-1/CD200-defined, CD4$^+$ memory T cell populations (T_{FH} vs. non-T_{FH}; 10^4 sorted cells, isolated as shown in Suppl. Fig. 1) obtained at the designated time points post-infection from Rh27617 (b; WT SIVmac239) and Rh25653 (c; SIVmac239Δnef) after 17 days of co-culture with CEMx174 cells (using flow cytometric analysis of intracellular SIV-Gag p27 to demonstrate CEMx174 cell infection; %Gag$^+$ cell shown). See Suppl. Fig. 3 for similar analysis of Rh26310 (WT SIVmac239) and Rh25714 (SIVmac239Δnef).

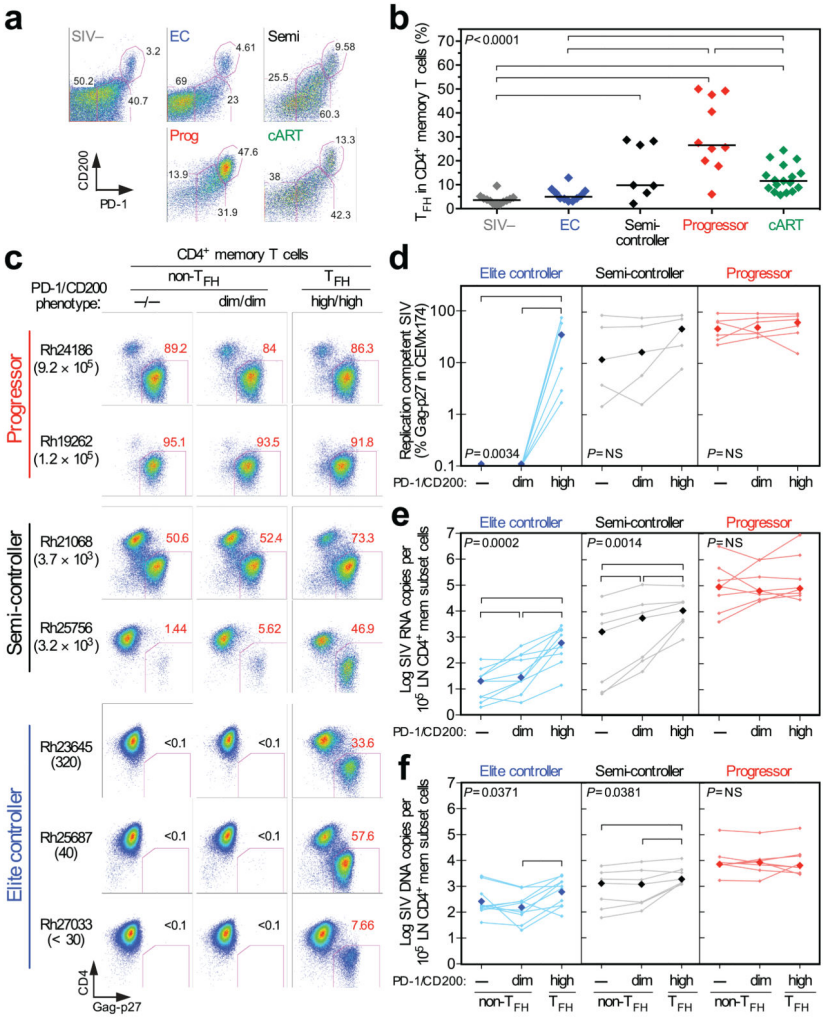

Figure 2. The distribution of productive WT SIV infection within CD4$^+$ memory T cell subsets in LN correlates with immune control

(a) Representative flow cytometric profiles showing the typical frequencies (%) of PD-1/CD200-defined subsets within the (CD95^{high}) CD4$^+$ memory T cell populations in LNs of SIV-, elite controller (EC), semi-controller (Semi), progressor (Prog) and cART-suppressed SIV-infected (cART) monkeys (see Suppl. Tables 1 and 2). (**b**) Relative frequencies of CD4$^+$ T_{FH} (CD200^{high}/PD-1^{high}) within the total CD4$^+$ memory T cell populations in LN of the designated monkey groups (black bars indicate the median value for each group). The Kruskal-Wallis test was used to determine the significance of overall differences in %CD4$^+$ T_{FH} among these monkey groups (p value shown), and if this p value was <0.05, the Wilcoxon rank-sum test was used to perform pair-wise analysis (brackets indicate p<0.05). (**c,d**) Detection of replication-competent SIVmac239 from sorted PD-1/CD200-defined CD4$^+$ memory T cell subsets of LNs from semi-controller and EC monkeys after 13 days of CEMx174 cell co-culture with 10^5 sorted LN cells, and from progressor monkeys after 17 days of CEMx174 cell co-culture with 10^4 sorted LN cells (note: fewer sorted CD4$^+$ memory T cells were available in progressor monkeys due to CD4$^+$ T cell depletion). Representative results are shown in (c), with plasma viral load (in SIV RNA copies/ml) at

the time of biopsy shown in parenthesis under the monkey identification numbers, and all analyses are shown in (d) with light colored lines delineating individual monkeys and bold diamond symbols delineating log median values of each group. The Friedman test was used to determine the significance of overall differences in detection of replication-competent SIV among the PD-1/CD200-defined $CD4^+$ memory T cell subsets (p values shown), and the Wilcoxon signed-rank test was used to perform pair-wise analysis when the Friedman p value was <0.05 (brackets indicate Wilcoxon signed-rank $p<0.05$). (**e,f**) Comparison of cell-associated SIV RNA (e) and DNA (f) levels in the same LN $CD4^+$ memory T cell subsets, with statistical analysis as described in (d).

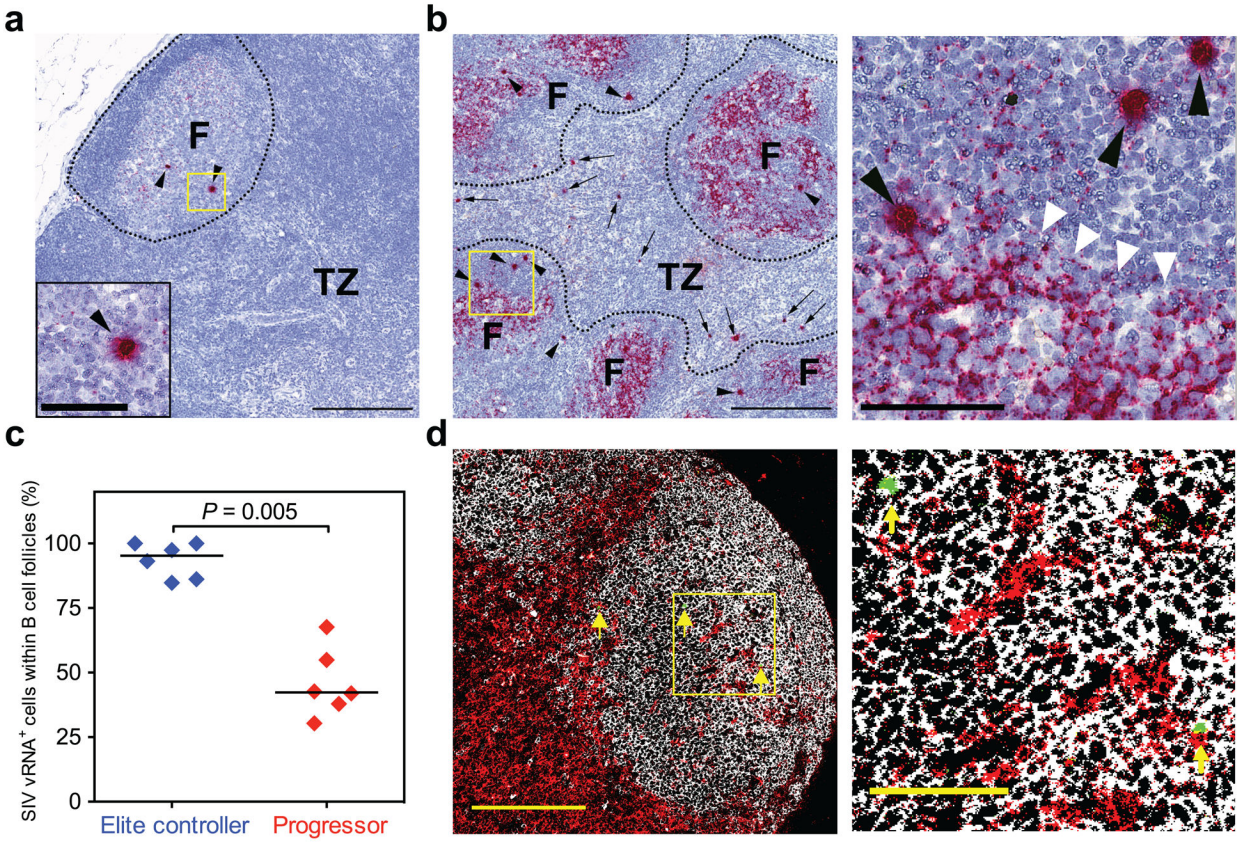

Figure 3. Productive SIV infection is anatomically restricted to B cell follicles in EC, but not progressor, monkeys

(**a,b**) Representative SIV (red) *in situ* hybridization (RNAscope) images from an EC monkey (a; Rh24827) vs. a chronically SIV-infected progressor (b; Rh-P383) with the yellow boxes indicating areas shown at higher magnification in either an insert (a; lower left) or a separate image at right (b). B cell follicles (F) are demarcated with dashed lines. Black arrows indicate all SIV RNA$^+$ lymphoid cells outside of follicles within the paracortical T cell zone (TZ), while arrowheads point to all SIV RNA$^+$ lymphoid cells within B cell follicles (note intense cell-centric SIV RNA signal within a single cell, consistent with productive infection), which are distinct from the well-characterized "lattice-like" filamentous pattern of extracellular FDC-bound virus that is also present within follicles (white arrowheads)[31]. Black scale bars = 100μm and 60μm in low and high magnification images, respectively. (**c**) Quantification of the percentage of total SIV RNA$^+$ cells within the LN of EC vs. progressor monkeys that are within B cell follicles (bars indicate median values). The Wilcoxon rank-sum test was used to determine the significance of differences in this percentage (p value shown). (**d**) Representative confocal micrograph of a LN section from an EC monkey (Rh24827) showing conventional *in situ* hybridization for SIV RNA (green) in combination with anti-CD20 (white) and anti-CD8 (red) antibody staining with the yellow box in the low magnification image (left) indicating the area shown at higher magnification at right. Yellow arrows indicate all productively SIV-infected cells in the image. Yellow scale bars = 200μm and 60μm in low and high magnification images, respectively.

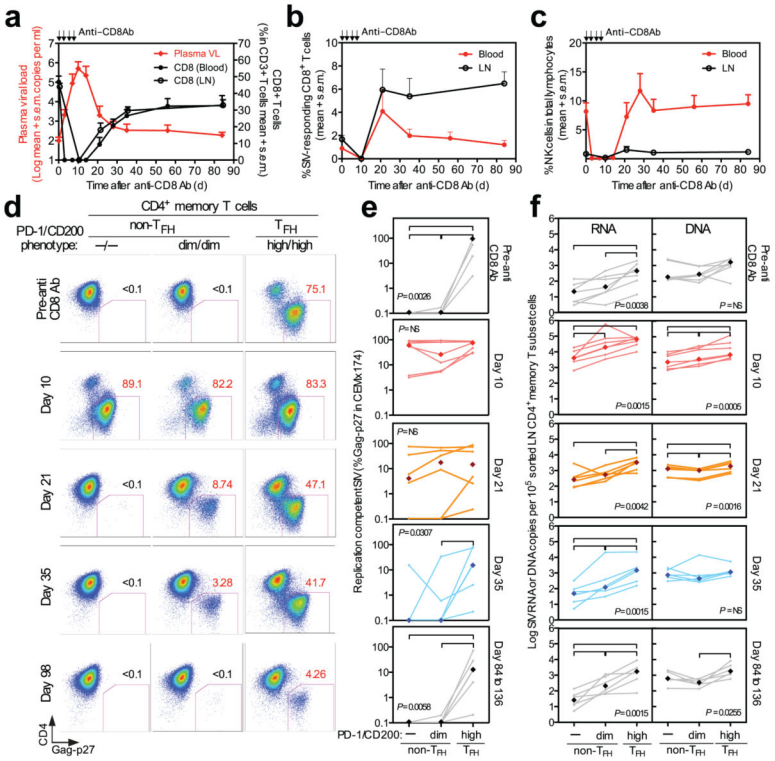

Figure 4. The restriction of productive SIV infection in CD4$^+$ T$_{FH}$ in EC LNs is lost with *in vivo* CD8$^+$ lymphocyte depletion

(a,b,c) Effect of CD8$^+$ lymphocyte depletion on plasma viral load and on frequencies of total CD3$^+$, CD8$^+$ T cells (a), SIV-specific CD8$^+$ T cells (b), by intracellular cytokine analysis, and total CD3$^-$CD8$^+$ NK cells (c) in peripheral blood and LN of EC monkeys. (**d**) Detection of replication-competent SIV from the designated sorted LN CD4$^+$ memory T cell populations (10^5 cells co-cultured with CEMx174 for 17 days) from a representative EC monkey (Rh26623) before and after anti-CD8 antibody treatment. (**e,f**) Quantitative analysis of the distribution of replication-competent SIV by CEMx174 co-culture analysis (e; 10^5 sorted LN cells; 17 to 22 days) and cell-associated SIV RNA and DNA levels by RT-PCR/PCR (f) among LN (PD-1/CD200-defined) CD4$^+$ memory T cell subsets before and after anti-CD8 antibody treatment of seven EC (see Suppl. Table 1) with light colored lines delineating individual monkeys and bold diamond symbols delineating log median values of each group. Note that one monkey, Rh27033, was taken to necropsy at day 10 post-depletion, so n = 6 at later time points. Statistical analysis was performed as described in Figure 2d (brackets indicate Wilcoxon signed-rank $p<0.05$).

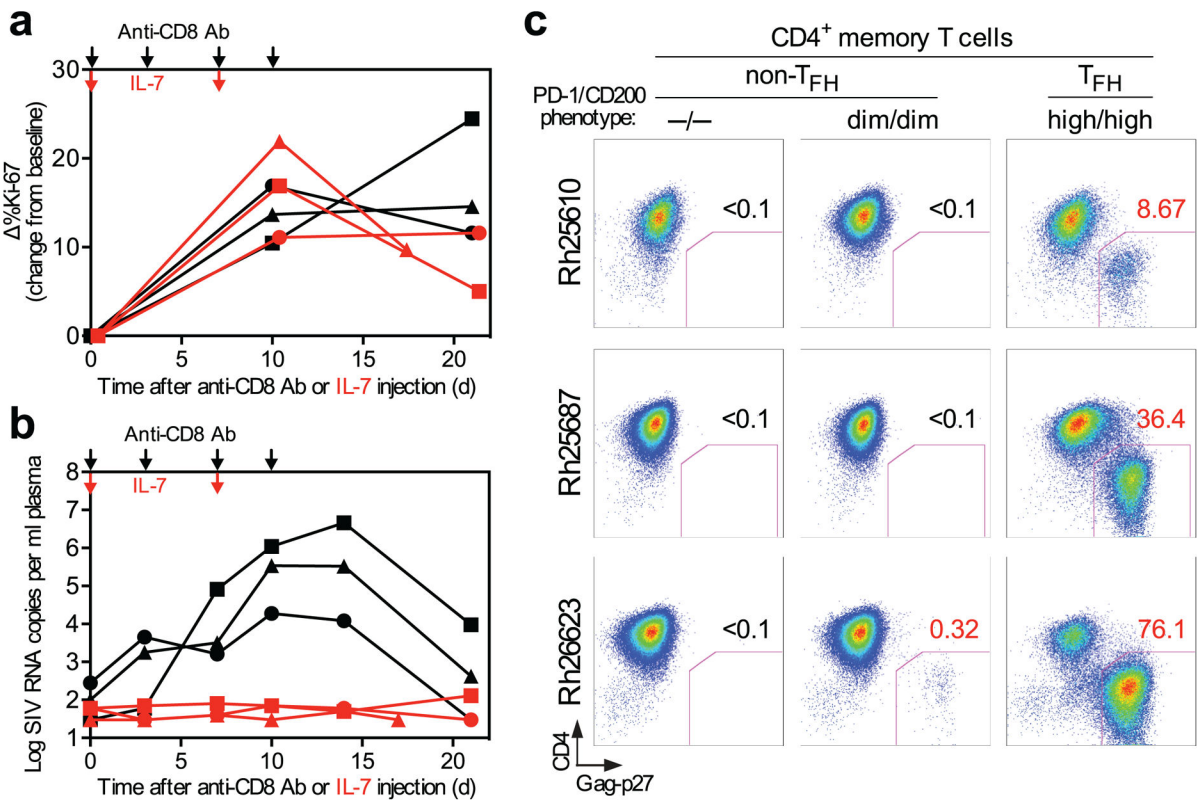

Figure 5. The restriction of productive SIV infection in CD4$^+$ T$_{FH}$ in EC LNs is not affected by activation of extra-follicular CD4$^+$ memory T cells with IL-7 administration

Three EC monkeys that had recovered both CD8$^+$ T cell counts and CD8$^+$ T cell-mediated SIV control (plasma viral load <100 copies/ml) 5–6 months after anti-CD8 antibody treatment were treated with recombinant rhesus IL-7 to activate extra-follicular CD4$^+$ memory T cells. (**a**) Comparison of the induction of the proliferation marker Ki-67 on LN non-T$_{FH}$ (PD-1$^{-/dim}$/CD200$^{-/dim}$) CD4$^+$ memory T cells from these 3 EC monkeys after CD8$^+$ lymphocyte depletion (black lines) vs. after IL-7 treatment (red lines; Δ%Ki-67 = post-treatment %Ki-67$^+$ - baseline %Ki-67$^+$). (**b**) Comparison of plasma viral load after CD8$^+$ lymphocyte depletion vs. after IL-7 treatment. (**c**) Detection of replication-competent SIV by CEMx174 co-culture analysis (10^5 sorted LN cells; 22 to 36 days) from sorted LN (PD-1/CD200-defined) CD4$^+$ memory T subsets of all 3 IL-7-treated EC monkeys 10 days after IL-7 treatment (the peak of non-T$_{FH}$ CD4$^+$ memory T cell proliferation). Note that in contrast to CD8$^+$ lymphocyte depletion (Fig. 4), induction of proliferation in extra-follicular CD4$^+$ memory T cells by IL-7 did not abrogate the restriction of productive SIV infection to CD4$^+$ T$_{FH}$ (e.g., did not result in an increase in productive infection of extra-follicular CD4$^+$ memory T cells).

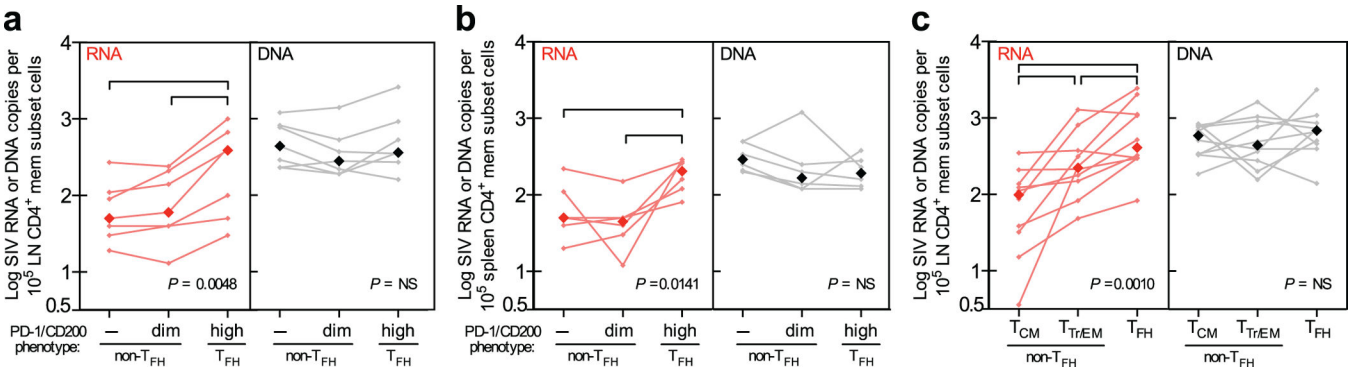

Figure 6. CD4$^+$ T_{FH} contain higher levels of cell-associated SIV RNA than non-T_{FH} CD4$^+$ memory T cells in SIV$^+$ RM with effective suppression of viral replication

(**a,b**) Comparison of the levels of cell-associated SIV RNA and DNA in sorted CD4$^+$ memory T cell subsets (PD-1$^-$ and PD-1^{dim} non-T_{FH} vs. PD-1^{high} T_{FH}; see Suppl. Fig. 1) from LN (a) and spleen (b) of Cohort #1 monkeys, which were chronically SIVmac251-infected prior to cART treatment and were assayed 4–6 months after cART initiation when plasma viral loads were ≤60 copies/ml (see Suppl. Table 2). (**c**) Comparison of the levels of cell-associated SIV RNA and DNA in sorted CD4$^+$ memory T cell subsets (T_{cm} and $T_{Tr/EM}$ vs. T_{FH}; see Suppl. Fig. 8) from LN of Cohort #2 monkeys, which were treated with cART 42 days post-infection with SIVmac239 and were assayed 6 months after cART initiation when plasma viral loads were ≤50 copies/ml (Suppl. Table 2). Light colored lines delineate individual monkeys and bold diamond symbols delineate log median values of each group. Statistical analysis was performed as described in Fig. 2d (brackets indicate Wilcoxon signed-rank $p<0.05$).